

Phase transition in random adaptive walks on correlated fitness landscapes

Su-Chan Park (박수찬)

The Catholic University of Korea, Bucheon 420-743, Korea

Ivan G. Szendro, Johannes Neidhart, and Joachim Krug

Institut für Theoretische Physik, Universität zu Köln, Köln 50937, Germany

(Dated: March 12, 2018)

We study biological evolution on a random fitness landscape where correlations are introduced through a linear fitness gradient of strength c . When selection is strong and mutations rare the dynamics is a directed uphill walk that terminates at a local fitness maximum. We analytically calculate the dependence of the walk length on the genome size L . When the distribution of the random fitness component has an exponential tail we find a phase transition of the walk length D between a phase at small c , where walks are short ($D \sim \ln L$), and a phase at large c , where walks are long ($D \sim L$). For all other distributions only a single phase exists for any $c > 0$. The considered process is equivalent to a zero temperature Metropolis dynamics for the random energy model in an external magnetic field, thus also providing insight into the aging dynamics of spin glasses.

PACS numbers: 87.23.Kg, 05.40.Fb, 75.10.Nr

I. INTRODUCTION

A population adapts to a new environment by accumulating beneficial mutations. To study evolution in general and adaptation in particular, the picture of a fitness landscape has proven to be helpful [1]. Here a unique fitness value is assigned to each genotype which reflects the mean number of viable offspring an individual with this genotype would produce. The mapping from genotype to fitness defines the fitness landscape. In this setting, adaptation is viewed as a hill-climbing process that the population performs on the fitness landscape.

The interest in fitness landscapes has been renewed in recent years as new techniques have made it possible to experimentally determine the fitness for combinatorially complete sets of multiple genetic loci [1, 2]. These experiments suggest that fitness landscapes typically contain a substantial amount of randomness but also display correlations that smoothen the landscape. In particular, many empirical fitness landscapes possess multiple local maxima, i.e. genotypes with fitnesses that are higher than those of all neighboring genotypes that can be reached by single-point mutations [3]. Such local fitness peaks slow down adaptation by temporarily trapping the population, and it is important to understand how long a population can evolve before it reaches a peak.

To address this question, we adopt the following simple but well established model, which captures the evolutionary dynamics in a regime of strong selection and weak mutation (SSWM) [4–7]. Consider a population of N individuals. Mutations occur with rate μ , which is chosen small in the sense that $N\mu \ll 1$. Selection is assumed to be strong enough that deleterious mutations rapidly go extinct. If a beneficial mutation appears, it has a finite probability to become dominant in the population, and this will happen before a second mutation can occur. Thus, in this regime, the whole population is almost always monomorphic, that is, genetically homogeneous.

By means of sequentially fixing beneficial mutations, the population “walks” uphill through the fitness landscape, until it reaches a local fitness maximum, at which only deleterious mutations are available. Despite its simplicity, the adaptive walk model has proven successful to describe microbial evolution in the laboratory [8–10].

A further common simplification is to suppose that all mutant genomes are of the same length L . Also, we only distinguish between genetic sites that are mutated and those that are not (diallelic loci, a common assumption in population genetics). This leads to an L -dimensional hypercubic genotype space of binary sequences $\mathcal{C} = (\dots, 0, \dots, 1, \dots)$, where zeros denote unmutated loci and ones mutated loci. To assign fitness values to genotypes, we consider the rough Mount Fuji (RMF) model, which is a simple yet versatile model of tunably rugged fitness landscapes [11–13] that has shown to be capable of capturing many features of empirical fitness landscapes [2, 12–14]. A realization of the landscape is constructed from independent and identically distributed random variables $\eta_{\mathcal{C}}$, which are combined with a linear fitness gradient to define the genotype fitness as

$$W(\mathcal{C}) = -cd(\mathcal{C}, \mathcal{C}_r) + \eta_{\mathcal{C}}. \quad (1)$$

Here the *reference sequence* $\mathcal{C}_r = (1, 1, \dots, 1)$ has all loci mutated and $d(\mathcal{C}, \mathcal{C}')$ is the Hamming distance between \mathcal{C} and \mathcal{C}' , with $d(\mathcal{C}, \mathcal{C}_r)$ being the number of zeros in \mathcal{C} . The probability density of $\eta_{\mathcal{C}}$ is $f(\eta_{\mathcal{C}})$ and the corresponding distribution function is $F(x) = \int_{-\infty}^x f(y)dy$. In the following we refer to $\eta_{\mathcal{C}}$ as the *random fitness component* [15].

When a walker is located at \mathcal{C} , a further step $\mathcal{C} \rightarrow \mathcal{C}'$ is performed by choosing \mathcal{C}' at random with equal probability from the set $\tilde{\mathcal{N}}(\mathcal{C}) = \{\mathcal{C}' | W(\mathcal{C}') > W(\mathcal{C}) \text{ and } d(\mathcal{C}', \mathcal{C}) = 1\}$ of single mutant neighbors with higher fitness. If this set is empty, \mathcal{C} is a local fitness maximum and the walker stops. We refer to this dy-

namics as the random adaptive walk (RAW) [16]. A key question in the theory of adaptive walks is the following [4, 6, 13, 16–21]: If the walker starts from the antipodal sequence $\mathcal{C}_a = (0, 0, \dots, 0)$ of \mathcal{C}_r , how many steps does it take before a fitness maximum is reached and the walk terminates? For the RAW on an uncorrelated random fitness landscape, corresponding to the RMF model with $c = 0$, the mean number of steps is known to be $D_{\text{RAW}} \approx \ln L + 0.099$ to leading order [17, 18]. On the other hand, when c is much larger than the standard deviation of the random fitness component in Eq. (1), the walker may take all L steps to the reference sequence with high probability.

The purpose of this paper is to clarify the nature of the transition between the regimes $D_{\text{RAW}} \sim \ln L$ and $D_{\text{RAW}} \sim L$ that occurs as c varies. We show that a phase transition at an intermediate value of c exists if and only if the distribution of the random fitness component has an exponential tail, and we characterize the transition in detail.

The RAW arises from the full SSWM dynamics as an approximation when fitness differences between neighboring genotypes are large [22]. The opposite case of small fitness differences has been considered in [5, 6, 19–21] for an uncorrelated landscape. We discuss the effect of using the full SSWM dynamics in Sec. III C.

II. RANDOM ADAPTIVE WALKS STARTING FROM THE ANTIPODE

A. Formal solution

Our analysis starts from writing formally the probability density $q_l(\mathcal{Y}_l)\theta_l$ that an adaptive walker takes at least l steps along a path \mathcal{Y}_l before it ends up at some local maximum. Here, \mathcal{Y}_l is the ordered set of random fitness components y_i of \mathcal{C}_i which have been visited by the walker at the i 'th step ($0 \leq i \leq l$), $\mathcal{Y}_l \equiv (y_0, y_1, \dots, y_l)$. We make the assumption that the distance to the reference sequence is strictly decreasing along the adaptive walk. Since the probability that a randomly chosen neighbor is located in the direction of the reference state is $1 - O(l/L)$, this assumption becomes exact as $L \rightarrow \infty$ as long as the walk distance l is $o(L)$. Within this assumption, the walker chooses a random genotype from $\mathcal{N}(\mathcal{C}_l) = \{\mathcal{C}' \in \tilde{\mathcal{N}} | d(\mathcal{C}', \mathcal{C}_r) = d(\mathcal{C}_l, \mathcal{C}_r) - 1\}$. The condition that y_{i-1} is smaller than $y_i + c$ for all $i = 1, 2, \dots, l$ in \mathcal{Y}_l will be called the walk condition and θ_l is 1 (0) if the walk condition is (not) satisfied.

Let us assume that the walker has taken l steps to \mathcal{C}_l with the random fitness component y_l . Since the walker can choose any genotype from $\mathcal{N}(\mathcal{C}_l)$, the probability density of y_{l+1} for a given y_l is $f(y_{l+1})/(1 - F(y_l - c))$ irrespective of the cardinality of $\mathcal{N}(\mathcal{C}_l)$, as long as it is not zero. Since $\mathcal{N}(\mathcal{C}_l)$ is empty with probability $F(y_l - c)^{L-l}$,

we get

$$q_{l+1}(\mathcal{Y}_{l+1}) = f(y_{l+1}) \frac{1 - F(y_l - c)^{L-l}}{1 - F(y_l - c)} q_l(\mathcal{Y}_l) \theta_{l+1}. \quad (2)$$

We next define $Q_l(y_l, L)$ as the probability (density) to take l steps and arrive at fitness $c(l - L) + y_l$. It is the integral of $q_l \theta_l$ over all y 's but y_l , $Q_l(y_l, L) = \int dy_0 \dots dy_{l-1} q_l(\mathcal{Y}_l) \theta_l$, and satisfies the recursion relation

$$Q_{l+1}(y, L) = f(y) \int_{-\infty}^{y+c} Q_l(x, L) \frac{1 - F(x - c)^{L-l}}{1 - F(x - c)} dx \quad (3)$$

with $Q_0(y, L) = f(y)$. The probability H_l that a walker takes at least l steps is obtained by integration over all endpoints $H_l = \int_{-\infty}^{\infty} Q_l(y, L) dy$, and the probability P_l that a walker takes exactly l steps is

$$P_l = H_l - H_{l+1} = \int_{-\infty}^{\infty} Q_l(y, L) F(y - c)^{L-l} dy. \quad (4)$$

Accordingly, the mean walk length can be calculated as

$$D_{\text{RAW}} = \sum_{l=1}^L l P_l = \sum_{l=1}^L H_l. \quad (5)$$

Although we have found a formal way of calculating D_{RAW} , it seems very difficult to find an analytic solution for arbitrary c and arbitrary $f(y)$ (see [18] for the solution in the case of $c = 0$). Rather than directly analyzing Eq. (3), we use the following approximation scheme. At first, we observe that for $L \rightarrow \infty$ with l kept finite, $H_l \rightarrow 1$ (likewise $P_l \rightarrow 0$), and $Q_l(y) \equiv Q_l(y, L = \infty)$ satisfies

$$Q_{l+1}(y) = f(y) \int_{-\infty}^{y+c} \frac{Q_l(x)}{1 - F(x - c)} dx, \quad (6)$$

with $Q_0(y) = f(y)$. According to Eq. (4), P_l is almost 0 as long as the region where $Q_l(y)$ is significant does not overlap with the region where $F(y - c)^{L-l}$ is significant in the sense that the product $Q_l(y) F(y - c)^{L-l} \ll 1$ for all y . A way to determine whether the two regions overlap is to check if $F(z_l - c)^{L-l}$ becomes of order unity, where z_l is the mean of $Q_l(y)$, or

$$z_l \equiv \int_{-\infty}^{\infty} y Q_l(y) dy. \quad (7)$$

Once the two regions are significantly overlapped, they remain so for larger l either by decreasing $L - l$ or by increasing z_l , and $Q_l(y, L)$ becomes significantly smaller than $Q_l(y)$. Since $F(x)$ approaches 1 as x gets larger and $F(z_l - c)^{L-l}$ can be significant when $1 - F(z_l - c) \sim O(1/(L - l))$, it suffices to estimate the solution of $F(z_l - c)^{L-l} = e^{-1}$ for an order of magnitude estimate of D_{RAW} .

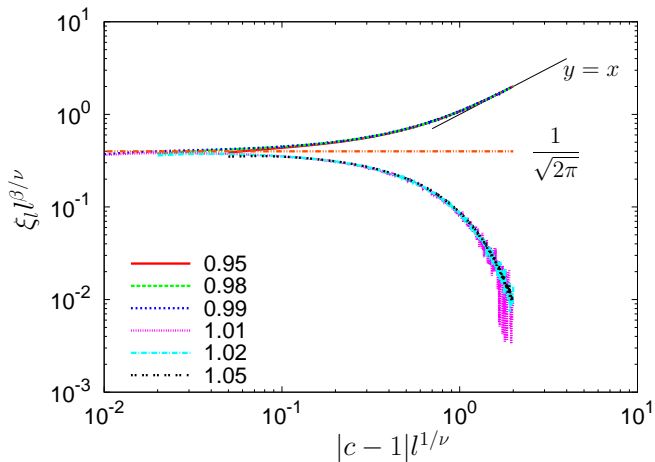


FIG. 1. (Color online) Scaling collapse plots of $\xi_l^{\beta/\nu}$ vs $|c-1|l^{1/\nu}$ with $\beta = 1$ and $\nu = 2$ for $c = 0.95, 0.98, 0.99, 1.01, 1.02,$ and 1.05 . Horizontal line corresponds to $\psi(0) = 1/\sqrt{2\pi}$ and the slanted line shows $y = x$, which confirms the scaling ansatz Eq. (13).

B. Exponential distribution

We apply the above approximation scheme to the case of an exponential distribution of random components, $f(x) = e^{-x}$, a common choice in the population genetics literature [23]. After a substantial amount of algebra (see Appendix A), we obtain

$$Q_l(y) = -\frac{d}{dy} \left(\sum_{n=0}^l y \frac{(y+cn)^{n-1}}{n!} e^{-y-cn} \right), \quad (8)$$

and z_l takes the form $1 + \sum_{k=1}^l \xi_k$, with (see Appendix B)

$$\xi_l = z_l - z_{l-1} \quad (9a)$$

$$= \frac{(cl)^{l+1} e^{-cl}}{l!} \int_0^\infty t e^{-ct} e^{(l-1)g(t)} dt \quad (9b)$$

$$= 1 - c - \frac{(cl)^{l+1} e^{-cl}}{l!} \int_{-1}^0 t e^{-ct} e^{(l-1)g(t)} dt, \quad (9c)$$

where $g(t) = \ln(1+t) - ct$. Note that $g(t)$ has a unique (local) maximum at $t_M = (1-c)/c$, such that it decreases (increases) for $t > t_M$ ($t < t_M$). In the case $c = 1$, ξ_l takes the simple form

$$\xi_l|_{c=1} = \frac{l^l e^{-l}}{l!} \sim \frac{1}{\sqrt{2\pi l}}. \quad (10)$$

For $c \neq 1$, we analyze the asymptotic behavior of ξ_l for large l . Since the integral domain in Eq. (9b) [(9c)] does not contain t_M if $c > 1$ [$c < 1$], we use the Laplace method of asymptotic analysis, applying it to Eq. (9b) for the case of $c > 1$ and Eq. (9c) for $c < 1$. When $l \gg 1$, the main contribution of the integral comes from the region around the maximum of $g(t)$ in the integral

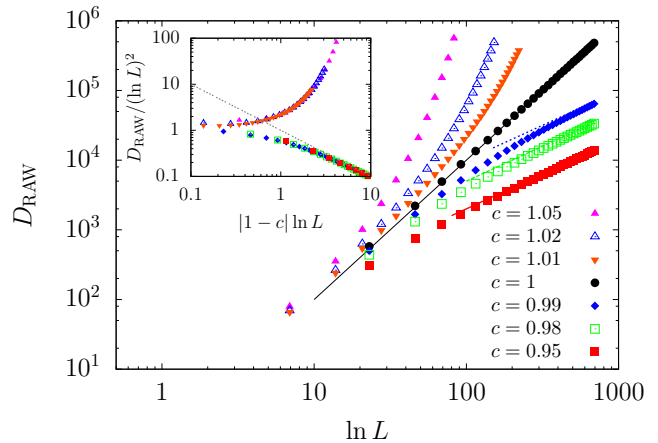


FIG. 2. (Color online) Plots of D_{RAW} vs $\ln L$ for $f(x) = e^{-x}$ and various choices of c on a double-logarithmic scale. The black line shows $(\ln L)^2$, while the other lines correspond to $\ln L/(1-c)$. (Inset) Scaling collapse plot of $D_{\text{RAW}}/(\ln L)^2$ against $|1-c|\ln L$ on a double-logarithmic scale. The straight line with slope -1 is drawn to show the $\ln L$ behavior of D_{RAW} for $c < 1$.

domain. Since the maximum of $g(t)$ in the integral domain of Eq. (9b) [(9c)] for $c > 1$ [$c < 1$] is at $t = 0$, we approximate $g(t) \approx (1-c)t$, which gives

$$\xi_l \approx \max(1-c, 0) + \frac{e^{-l(c-1-\ln c)}}{\sqrt{2\pi l}} \frac{c}{(c-1)^2 l}, \quad (11)$$

where we have used Stirling's formula. Since $c-1-\ln c > 0$ for $c \neq 1$, ξ_l approaches $\max(1-c, 0)$ exponentially fast. Also when $|c-1| \ll 1$, we can approximate $c-1-\ln c \approx (c-1)^2/2$, suggesting a scaling form

$$\xi_l(c, l) = l^{-\beta/\nu} \psi((c-1)l^{1/\nu}), \quad (12)$$

where, in the standard notation of critical phenomena, $\beta = 1$ and $\nu = 2$. Combining the approximations for the cases of $c \neq 0$ with Eq. (10), the asymptotic behavior of $\psi(x)$ takes the form

$$\psi(x) = \begin{cases} 1/\sqrt{2\pi}, & x \rightarrow 0, \\ e^{-x^2/2}/(\sqrt{2\pi}x^\nu), & x \rightarrow \infty, \\ |x|^\beta + e^{-x^2/2}/(\sqrt{2\pi}x^\nu), & x \rightarrow -\infty. \end{cases} \quad (13)$$

To confirm the scaling, we calculated ξ_l for different values of c using Monte Carlo simulations and the scaling plot is drawn in Fig. 1. We emphasize that the results of the Monte Carlo simulations are in complete agreement with those obtained by direct numerical integration of Eq. (9). Thus, we obtain

$$z_l = 1 + \sum_{m=1}^l \xi_m \sim \begin{cases} (1-c)l, & c < 1, \\ \sqrt{2l/\pi}, & c = 1, \\ \text{finite}, & c > 1. \end{cases} \quad (14)$$

Since the distribution of the random fitness component is exponential, $Q_l(y)$ is not expected to have a fat tail for

large l . To confirm this expectation, we calculated the standard deviation σ_l of $Q_l(y)$ and found that $\sigma_l \sim O(\sqrt{l})$ for $c \leq 1$ and $\sigma_l \sim O(1)$ for $c > 1$; see Appendix B. This implies that for $c < 1$, $Q_l(y)$ can be well approximated by $\delta(y - z_l)$ for large l and P_l becomes significant when $l \sim (\ln L)/(1-c)$. For $c = 1$, z_l and σ_l are comparable and $Q_l(y)$ cannot be approximated by a δ function. However, we expect that when $\ln F(z_l + \sigma_l) \sim -\ln L$, P_l starts to become significant. Hence, we conclude that

$$D_{\text{RAW}} \propto \begin{cases} \ln L/(1-c), & c < 1, \\ (\ln L)^2, & c = 1, \\ O(L), & c > 1. \end{cases} \quad (15)$$

In the limit $L \rightarrow \infty$ the ratio D_{RAW}/L remains finite for $c > 1$ but approaches 0 for $c \leq 1$, which means there is a phase transition at the critical point $c^* = 1$. For $c = 0$ we recover the result of [18]. In Fig. 2 we compare our prediction to simulation results, finding excellent agreement. Furthermore, Eq. (15) suggests that plots of $D_{\text{RAW}}/(\ln L)^2$ vs $(1-c)\ln L$ can be collapsed into a single curve, which is confirmed in the inset of Fig. 2. Because the dynamics is invariant under the multiplication of the fitness $W(C)$ by a constant factor, for a general exponential distribution $f(x) = a^{-1}e^{-x/a}$ the critical point is given by the mean of the distribution, $c^* = a$, and the walk length for $c < c^*$ is of the order of $\ln L/(1-c/a)$.

C. Other distributions

Now we argue that the nature of the phase transition is determined solely by the tail behavior of $f(y)$ and only exponential tails can induce a phase transition in the large L behavior as a function of c . Let us revisit Eq. (6) and consider distributions $f(y)$ that are supported on the entire real axis. Multiplying both sides of Eq. (6) with y and performing a partial integration, one can then derive the relation

$$z_{l+1} - z_l = \int_{-\infty}^{\infty} \frac{Q_{l+1}(y)}{h(y)} dy - c, \quad (16)$$

where $h(y)$ is the hazard function defined as

$$h(y) \equiv \frac{f(y)}{1 - F(y)}. \quad (17)$$

Let us now *assume* that $z_l \rightarrow \infty$ as $l \rightarrow \infty$ and that $Q_l(y)$ is reasonably concentrated, as was explicitly shown above for the case when $f(y)$ is exponential. Then we can replace the hazard function in the integral on the right hand side of Eq. (16) with its asymptotic form for large arguments. Distributions with exponential tails are the only ones for which the hazard function approaches a constant for large y , specifically $\lim_{y \rightarrow \infty} h(y) = a^{-1}$ for $-\ln f(x) = a^{-1}x + o(x)$. Inserting this into Eq. (6) and using the fact that Q_l is normalized, we arrive at

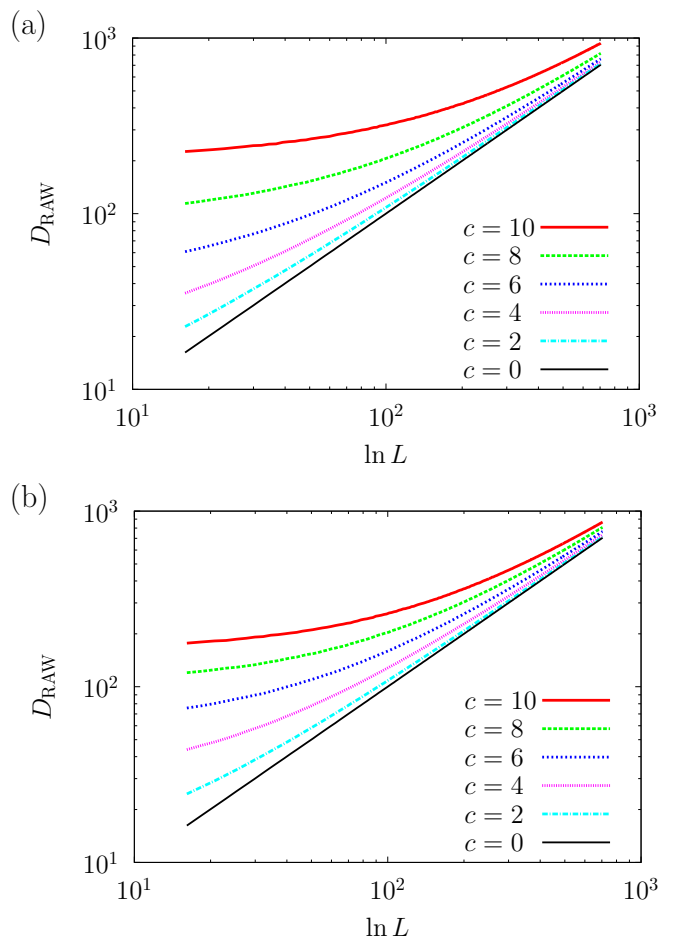


FIG. 3. (Color online) Double-logarithmic plots of D_{RAW} vs $\ln L$ for various choices of c (a) for the WD with $\alpha = \frac{1}{2}$ and (b) for the GPD with $\kappa = 0.5$. The case of $c = 0$, which is exactly solvable, is also drawn for comparison. $D_{\text{RAW}} \sim \ln L$ in the large L limit, independently of c .

$z_{l+1} - z_l \approx a - c$, showing that $z_l \approx (a - c)l$ for $c < a$, while for $c > a$ the assumption that z_l diverges is inconsistent. These results reproduce the previous analysis for the purely exponential distribution [but note that in this case the relation Eq. (16) does not strictly hold, because the support of the distribution is bounded on the left].

For a tail of the form $\ln f(y) \sim -y^\alpha$, the asymptotic behavior of the hazard function is $h(y) \sim y^{\alpha-1}$. Thus, the assumption that z_l diverges is consistent only for $\alpha < 1$. Provided Q_l is sufficiently narrow we can estimate the integral on the right hand side to be of order $z_l^{1-\alpha}$; hence, $z_{l+1} - z_l \approx z_l^{1-\alpha} - c$. The asymptotic solution is $z_l \sim l^{1/\alpha}$ for any c , and it is straightforward to check that this implies that the walk length is always proportional to $\ln L$. Similarly, for a power law tail $f(y) \sim y^{-(\mu+1)}$ the hazard function $h(y) \sim \frac{1}{y}$, which leads to an exponential growth of z_l for any c , and again to a walk length that is logarithmic in L . Conversely, for distributions with tails thinner than exponential such as the case $\alpha > 1$ mentioned above, the integral on the right hand side of

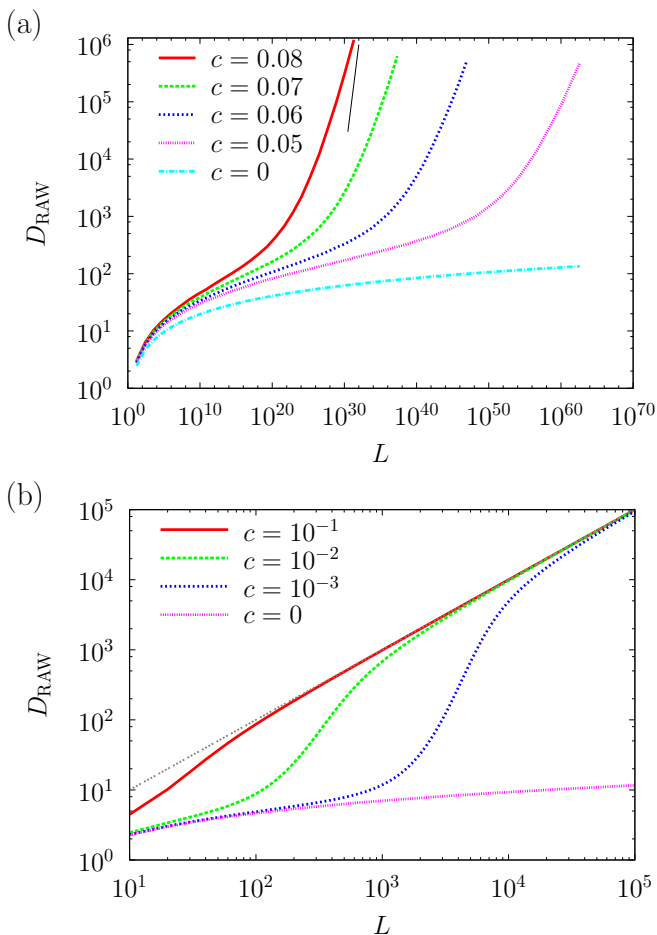


FIG. 4. (Color online) Double logarithmic plots of D_{RAW} vs L for various choices of c (a) for the WD with $\alpha = 2$ and (b) for the GPD with $\kappa = -1$. The line segment in (a) and the straight line in (b) show the line $y \propto x$. The case of $c = 0$ which is exactly solvable is also drawn for comparison. D_{RAW} increases linearly in L in the large L limit, independently of c .

Eq. (16) never becomes large and the behavior is dominated by the negative term c for any $c > 0$, leading to a walk length that is linear in L . Only when $c = 0$ does one obtain $z_l \sim l^{1/\alpha}$, which implies that the walk length is again $O(\ln L)$, consistent with the results in [18]. Thus, we conclude that a non-trivial transition is possible only for exponential tails.

To check our prediction that no phase transition occurs if the tail of the distribution is not exponential, we numerically calculated D_{RAW} for the Weibull distribution (WD) $F(x) = 1 - e^{-x^\alpha}$, with $\alpha = 0.5$ and $\alpha = 2$, and for the generalized Pareto distribution (GPD), $F(x) = 1 - (1 + \kappa x)^{-1/\kappa}$, with $\kappa = 0.5$ and $\kappa = -1$. The case of $\kappa = -1$ corresponds to a uniform distribution.

As predicted, for the two cases where the tail of the distribution falls off slower than exponentially, i.e. WD with $\alpha = 0.5$ and GPD with $\kappa = 0.5$, D_{RAW} will eventually, in the limit of large L , always grow as $\ln L$, irrespective of the value of c ; see Fig. 3. For the distributions that

fall off faster than exponentially, i.e. WD with $\alpha = 2$ and GPD with $\kappa = -1$, we verify that D_{RAW} grows as $\ln L$ for $c = 0$ and as L for any $c > 0$; see Fig. 4.

III. GENERALIZATIONS

In this section, we discuss three variants of the model. In Sec. III A, we ask how changing the initial condition of the RAW affects the phase transition point. To this end, we abandon the assumption that the walker always takes steps toward the reference genotype. In Sec. III B, we discuss how the phase transition is modified when the linear fitness gradient in the RMF model is replaced with a general nonlinear function of the distance to the reference sequence, focusing on the case where the initial genotype is the antipode. Finally in Sec. III C, we consider the full SSWM dynamics where a step towards a fitter genotype, rather than occurring with certainty, is accepted with a fixation probability π_f that depends on the fitness difference between the new and the old sequences. Most of the discussion in this section parallels the arguments in Sec. II C. For convenience, we use the same notation as in Sec. II A for similar quantities in this section.

A. Different initial condition

Up to now, the initial genotype was taken to be the antipode of the reference sequence. In this section, the walker is assumed to start from a genotype at Hamming distance \mathcal{L} from the reference sequence, where $0 \leq \mathcal{L} \leq L$. When considering the infinite L limit, the ratio \mathcal{L}/L is kept finite; that is,

$$\phi \equiv \lim_{L \rightarrow \infty} \frac{\mathcal{L}}{L}. \quad (18)$$

Note that the value of ϕ for the case considered in the previous section is 1.

Suppose that the walker has already taken l steps and the Hamming distance of the l th genotype, say \mathcal{C}_l , from the reference sequence is $d(\mathcal{C}_r, \mathcal{C}_l) = \ell$. Clearly, there are ℓ neighbors in the direction towards the reference sequence (the *uphill* direction for short) and $L - \ell$ neighbors in the direction away from the reference sequence (the *downhill* direction) [13]. Although at least one of the L neighbors of the current genotype was encountered previously during the walk, the correlation arising due to the previously assigned fitness value is negligible because the probability that a mutation reverts to a previously observed genotype is negligibly small as long as L is very large [13, 18]. Hence, it is a good approximation to assume that the walker sees a new genotypic environment after each step. Within this assumption, we can write a recursion relation similar to Eq. (3).

If the random part of $W(\mathcal{C}_l)$ is x , the probability $P_{\uparrow}(n_1)$ that there are n_1 beneficial mutations in the uphill di-

rection and the probability $P_{\downarrow}(n_{-1})$ that there are n_{-1} beneficial mutations in the downhill direction are

$$P_{\uparrow}(n_1) = \binom{\ell}{n_1} (1 - F(x - c))^{n_1} F(x - c)^{\ell - n_1}, \quad (19)$$

$$P_{\downarrow}(n_{-1}) = \binom{L - \ell}{n_{-1}} (1 - F(x + c))^{n_{-1}} F(x + c)^{L - \ell - n_{-1}}.$$

Note that the probability of $n_1 = n_{-1} = 0$, which corresponds to the probability that the walker stops at C_l , is $F(x - c)^\ell F(x + c)^{L - \ell}$. When there are n_1 and n_{-1} beneficial mutations in the uphill and downhill directions, respectively, the probability that the walker takes a step toward the reference sequence [the antipode] is n_1/n [n_{-1}/n], where $n \equiv n_1 + n_{-1}$. Hence the probability density $\rho(y|x)$ that the random part of the next genotype is y under the condition that the walker will take a step is

$$\rho(y|x) = \sum_{\sigma=\pm 1} \sum_{n=1}^L \frac{n_\sigma}{n} \frac{f(y)\theta(y - x + \sigma c)}{1 - F(x - \sigma c)} P_{n_1, n_{-1}}, \quad (20)$$

where the summation over n stands for that over $n_1 = 0, \dots, \ell$ and $n_{-1} = 0, \dots, L - \ell$ with $n = n_1 + n_{-1} > 0$, $\theta(x)$ is the Heaviside step function, and $P_{n_1, n_{-1}} \equiv P_{\uparrow}(n_1)P_{\downarrow}(n_{-1})$. Hence we get the recursion relation

$$Q_{l+1}(y, L) = \int_{-\infty}^{\infty} \rho(y|x) Q_l(x, L) dx. \quad (21)$$

As in Sec. II A, we now assume that L is very large and l is small in the sense that $l/L \rightarrow 0$ and $\ell/L \rightarrow \phi$ under the $L \rightarrow \infty$ limit. Within this assumption, the probability distributions of n_1 and n_{-1} are sharply peaked around $L\phi F(x - c)$ and $L(1 - \phi)F(x + c)$, respectively. Hence $Q_l(y) = \lim_{L \rightarrow \infty} Q_l(y, L)$ and its mean z_l satisfy the recursion relations

$$Q_{l+1}(y) = f(y) \int_{-\infty}^{\infty} dx Q_l(x) \times \frac{\theta(y - x + c) + \varphi \theta(y - x - c)}{1 - F(x - c) + \varphi [1 - F(x + c)]}, \quad (22)$$

$$z_{l+1} - z_l = \int_{-\infty}^{\infty} \frac{Q_{l+1}(y)}{h(y)} dy - c \int_{-\infty}^{\infty} dx Q_l(x) \frac{1 - \varphi \tilde{F}(x, c)}{1 + \varphi \tilde{F}(x, c)}, \quad (23)$$

where $\varphi = (1 - \phi)/\phi$ and $\tilde{F}(x, c) = [1 - F(x + c)]/[1 - F(x - c)]$. In the derivation of Eq. (23) it is implicitly assumed that the support of $f(x)$ extends over the whole real axis. Note that when $\phi = 1$, the above equations reduce to Eqs. (6) and (16), respectively. By symmetry, the case of $\phi = 0$ corresponds to a walker starting at the antipodal sequence with $c < 0$, and it is clear from the results of the previous section that the walk distance cannot be larger than for $c = 0$. So we restrict ourselves to the case of $c > 0$ and $\phi > 0$ in the following.

As in Sec. II C, we first assume that z_l diverges as $l \rightarrow \infty$ and that $Q_l(x)$ is highly peaked around z_l for

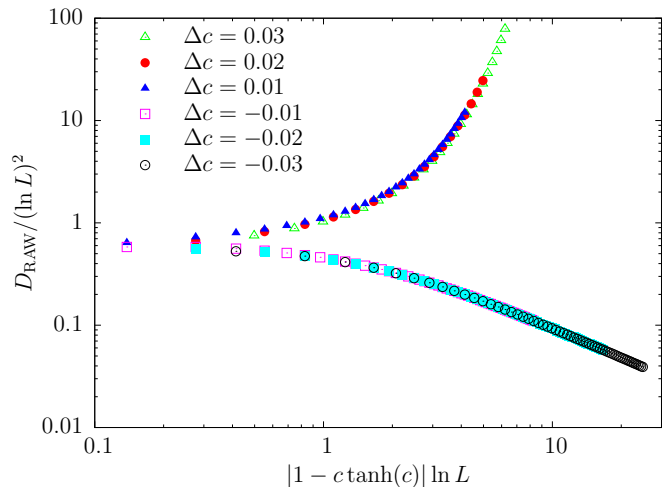


FIG. 5. (Color online) Finite size scaling collapse plot of $D_{\text{RAW}}/(\ln L)^2$ vs $|1 - c \tanh(c)| \ln L$ for $c = \tilde{c} + \Delta c$ with $\Delta c = 0.03, 0.02, 0.01$ (top data sets) and $-0.01, -0.02, -0.03$ (bottom data sets), where $\tilde{c} = 1.199\ 678\ 640$ is the solution of Eq. (25) with $\varphi = 1$.

sufficiently large l . When the tail is exponential, that is, $-\ln[1 - F(x)] = a^{-1}x + o(x)$ and $h(y) = 1/a + o(1)$, Eq. (23) for large l becomes

$$z_{l+1} - z_l \approx a - c \frac{1 - \varphi e^{-2c/a}}{1 + \varphi e^{-2c/a}}. \quad (24)$$

Hence the assumption that z_l diverges breaks down if $c > a\tilde{c}$, where \tilde{c} is the (positive) solution of the equation

$$\varphi = \frac{\tilde{c} - 1}{\tilde{c} + 1} e^{2\tilde{c}}. \quad (25)$$

Thus, we conclude that the phase transition point depends on ϕ . When $\phi = 1$, we get $\tilde{c} = 1$, as before, and when $\phi \ll 1$, \tilde{c} diverges logarithmically with ϕ as $\tilde{c} \sim -\frac{1}{2} \ln \phi$.

To support the above conclusion, we present simulation results for $\varphi = 1$ ($\phi = \frac{1}{2}$), with $f(x) = e^{-x}$ in Fig. 5. The predicted transition point for $\varphi = 1$ is determined by the equation $1 - \tilde{c} \tanh(\tilde{c}) = 0$, whose solution is $\tilde{c} \approx 1.199\ 678\ 640$. Close to this value we expect a finite size scaling collapse when $D_{\text{RAW}}/(\ln L)^2$ is plotted as a function of $|1 - c \tanh(c)| \ln L$, which is indeed the case as shown in Fig. 5.

The analysis for other distributions proceeds analogously to Sec. II C. If $-\ln[1 - F(x)] = o(x)$ (slower than exponential decay), $\tilde{F}(z, c) \rightarrow 1$ as $z \rightarrow \infty$. Then Eq. (23) asymptotically becomes Eq. (16) with c replaced with $c(2\phi - 1)$, which implies that the walk distance is always $O(\ln L)$. If $-1/\ln[1 - F(x)] = o(1/x)$ (faster than exponential decay), $\tilde{F}(z, c) \rightarrow 0$ as $z \rightarrow \infty$ and Eq. (23) asymptotically becomes Eq. (16), which implies that the walk distance is $O(L)$ as long as $c > 0$.

To sum up, the initial condition of the RAW can affect the location of the critical point for the case of distri-

butions with an exponential tail, but does not otherwise change the existence or nature of the phase transition.

B. Nonlinear deterministic fitness function

The linear fitness gradient in Eq. (1) implies that, in the absence of the random fitness component ηc , each mutation away from the reference sequence would decrease fitness by the same amount c , and that the effects of different mutations combine additively. However, in many cases it is observed that the effect of a mutation depends on whether or not other mutations have occurred previously, a phenomenon referred to as epistasis [24, 25].

To model such situations, we replace the linear deterministic part in Eq. (1) by a general function of the distance to the reference sequence and ask how the phase transition is affected by this modification. Since the main purpose of this section is to explain the qualitative change in the nature of the transition, we restrict ourselves to the case when the RAW starts at the antipodal sequence. As in Sec. II, we assume that the walker always takes steps toward the reference sequence.

If the fitness of the sequence takes the form (recall that \mathcal{C}_a is the antipode of the reference sequence)

$$W(\mathcal{C}) = k_{d(\mathcal{C}, \mathcal{C}_a)} + \eta c, \quad (26)$$

it is straightforward to show that the recursion relation Eq. (16) for z_l generalizes to

$$z_{l+1} - z_l = \int_{-\infty}^{\infty} \frac{Q_{l+1}(y)}{h(y)} dy - \Delta k_l, \quad (27)$$

with $\Delta k_l \equiv k_{l+1} - k_l$. In the following we assume that k_l is an increasing function of l such that $\Delta k_l > 0$. As explained in Sec. II A, the walk length D_{RAW} will be estimated from the solution of

$$F(z_l - \Delta k_l)^{L-l} = e^{-1}. \quad (28)$$

To be concrete, let us consider distributions of the form $\ln f(y) \approx -a^{-1}y^\alpha$, which gives $h(y) \approx a^{-1}\alpha y^{\alpha-1}$ for sufficiently large y . If we assume that z_l diverges with l and $Q_l(x)$ is well approximated by $\delta(x - z_l)$ for sufficiently large l , Eq. (27) becomes

$$z_{l+1} - z_l \approx \frac{1}{h(z_l)} - \Delta k_l \approx \frac{a}{\alpha} z_l^{1-\alpha} - \Delta k_l. \quad (29)$$

Hence, the necessary condition for z_l to diverge with l is $h(z_l)\Delta k_l < 1$, or $az_l^{1-\alpha} > \alpha\Delta k_l$. If indeed $1/h(z_l) \gg \Delta k_l$ for sufficiently large l , then the asymptotic form of Eq. (29) becomes

$$1 \approx h(z) \frac{dz}{dl} = -\frac{d}{dl} \ln(1 - F[z(l)]) \quad (30)$$

which gives

$$1 - F[z(l)] \approx e^{-l}. \quad (31)$$

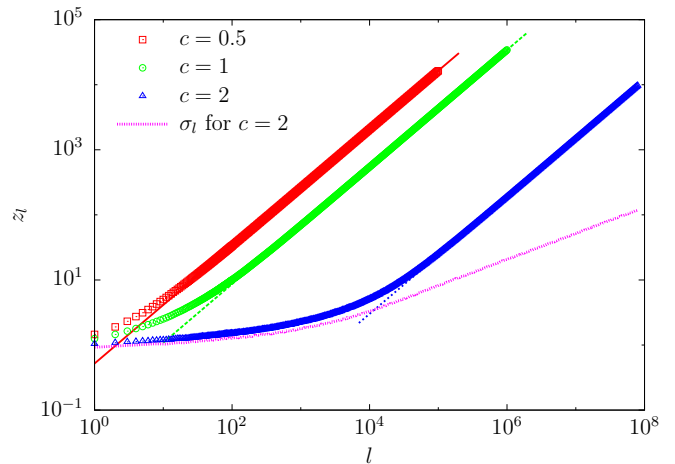


FIG. 6. (Color online) Double-logarithmic plots of mean z_l (symbols) and standard deviation σ_l (bottom line) of the distribution $Q_l(x)$ against l for a nonlinear deterministic fitness function $\Delta k_l = cl^{b-1}$ ($k_0 = 0$) with $b = 0.9$. Lines show the asymptotic power law $z_l = (Al)^b$ with the prefactor A given by the numerical solution of Eq. (34).

Here $z(l)$ is an analytic continuation of z_l , and it follows from the assumed shape of F that $z(l) \sim l^{1/\alpha}$. Since $\Delta k_l \ll 1/h(z_l) = O(z_l^{1-\alpha}) \ll z_l$ under the present assumption, we can replace $F(z_l - \Delta k_l)$ with $F(z_l)$ in the condition Eq. (28) and it follows from Eq. (31) that $D_{\text{RAW}} \sim O(\ln L)$.

To see when this scenario applies, we take k_l to increase as a power law [26],

$$\Delta k_l = cl^{b-1} + o(l^{b-1}), \quad (32)$$

where $b = 1$ corresponds to the linear fitness gradient. Then the condition $h(z_l)\Delta k_l \gg 1$ is fulfilled when $\alpha < 1/b$. That is, for distributions with the tail decaying more slowly than $e^{-x^{1/b}}$, the mean walk distance is always $O(\ln L)$ irrespective of the value of c . On the other hand, if $\alpha > 1/b$, a trial solution $z_l \sim l^{1/\alpha}$ is contradictory to Eq. (29), which suggests that the walk distance is $O(L)$ for any $c > 0$.

In analogy with the linear case $b = 1$, a possible phase transition is anticipated when $\alpha = 1/b$. In this case, the asymptotic equation becomes

$$z_{l+1} - z_l = abz_l^{(b-1)/b} - cl^{b-1}. \quad (33)$$

If we assume that $z_l \approx (Al)^\gamma$, the leading terms on both sides of Eq. (33) are consistent when $\gamma = b$, and the prefactor A satisfies the equation

$$abA^{b-1} - bA^b = c. \quad (34)$$

Inspection of Eq. (34) reveals qualitatively different behaviors for the cases $b > 1$ and $b < 1$, respectively. In fact, the case of $b > 1$ turns out to require a different analysis which is beyond the scope of this paper. Hence

we limit ourselves to $b < 1$ and defer the discussion about the case of $b > 1$ to a future publication.

For $b < 1$, a unique positive solution of Eq. (34) for A can be found for any $c > 0$, which implies that the walk length is always logarithmic and a phase transition does not occur. To check the validity of the assumptions leading to Eq. (27), we have determined $Q_l(x)$ and its moments by direct simulation. Figure 6 strongly supports that z_l asymptotically diverges as l^b with the prefactor predicted by Eq. (34) for any $c > 0$ when $b < 1$. Furthermore, it is clear from Fig. 6 that the standard deviation σ_l of Q_l is negligibly small compared to z_l for sufficiently large l , which supports the assumption that $Q_l(x)$ is well described by a δ function $\delta(x - z_l)$ in the asymptotic regime.

Quite generally, we see that the behavior of the walk distance is strongly affected by the deterministic fitness profile and its interplay with the tail of the distribution of the random fitness component. It is unclear at present whether a phase transition as a function of c is possible for fitness profiles other than the linear one.

C. Finite fixation probability

The probability of fixation of a beneficial mutation is a function $\pi_f(s)$ of its selection coefficient, which in the present setting is simply the fitness difference $s = W(\mathcal{C}') - W(\mathcal{C})$ between the mutant genotype \mathcal{C}' and the resident genotype \mathcal{C} . The functional form of $\pi_f(s)$ depends on the details of the underlying population dynamics. For the particular case of Wright-Fisher dynamics, where populations evolve in discrete generations and the number of offspring of an individual is Poisson distributed [27], the fixation probability is well approximated by the expression $\pi_f(s) = 1 - e^{-2s}$ first derived by Kimura [28]. For small s this reduces to Haldane's classic result $\pi_f \approx 2s$ [29], which is exact in this limit, but for large s the true fixation probability of the Wright-Fisher model approaches unity somewhat more slowly, as $1 - \pi_f(s) \sim e^{-s}$ [27]. For this reason we here use a slight generalization of the Kimura formula, which reads

$$\pi_f(s) = 1 - e^{-\lambda s}. \quad (35)$$

For $\lambda \rightarrow \infty$ we thus recover the case of the RAW studied in the previous sections, whereas for $\lambda \rightarrow 0$ we obtain the Haldane-type fixation dynamics that is usually considered in the SSWM literature [4–7, 19–21].

As before, we consider the limit of infinite L . In this case, we expect that effectively all possible values of the random fitness components should appear with their appropriate weights. Since the fixation probability of a beneficial mutation with random component y in the uphill direction is $\pi_f(y - x + c)$, where x is the random component of the current genotype, we find the recursion

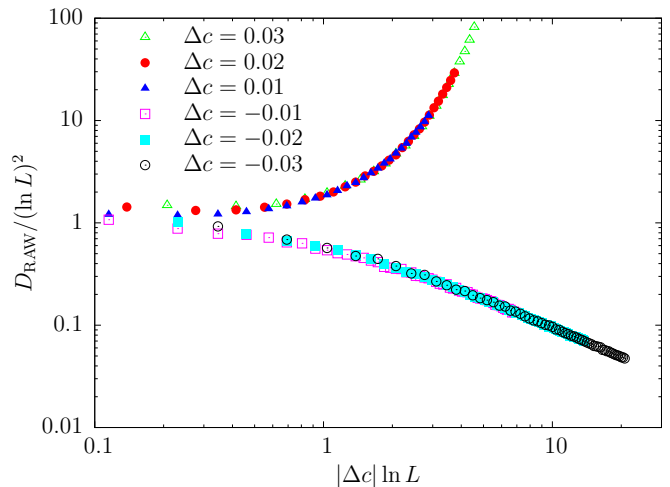


FIG. 7. (Color online) Finite size scaling collapse plot of $D_{\text{RAW}}/(\ln L)^2$ vs $|\Delta c| \ln L$ for $\Delta c = c - \frac{4}{3}$, with $\Delta c = 0.03, 0.02, 0.01$ (top data sets) and $-0.01, -0.02, -0.03$ (bottom data sets). The fixation probability Eq. (35) was used with $\lambda = 2$, and the distribution of the random fitness component is exponential with unit mean.

relation for $Q_l(y)$ as [19, 20, 22]

$$Q_{l+1}(y) = \int_{-\infty}^{y+c} \frac{\pi_f(y-x+c)f(y)}{\int_{x-c}^{\infty} \pi_f(z-x+c)f(z)dz} Q_l(x) dx \quad (36)$$

Again, we are looking for a condition for z_l to diverge. Assuming that it diverges and that $Q_l(x)$ is highly peaked around z_l , we get

$$\begin{aligned} z_{l+1} &= \int_{-\infty}^{\infty} dx Q_l(x) \int_{x-c}^{\infty} dy \frac{\pi_f(y-x+c)yf(y)}{\int_{x-c}^{\infty} \pi_f(z-x+c)f(z)dz} \\ &\approx z_l - c + \int_{z_l-c}^{\infty} \frac{\tilde{h}(y)}{\tilde{h}(z_l-c)} dy \end{aligned} \quad (37)$$

where $\tilde{h}(y) \equiv \int_y^{\infty} \pi_f(z - z_l + c)f(z)dz$ and we have used $Q_l(x) \approx \delta(x - z_l)$.

One can readily evaluate the right hand side of Eq. (37) for the fixation probability Eq. (35) and an exponential distribution $f(x) = e^{-x/a}$, which gives

$$z_{l+1} - z_l = a \frac{\lambda a + 2}{\lambda a + 1} - c. \quad (38)$$

This equation is consistent with a diverging solution for $c < a(\lambda a + 2)/(\lambda a + 1)$, and we conclude that the transition point is $c^* = a(\lambda a + 2)/(\lambda a + 1)$. Note that the $\lambda \rightarrow \infty$ limit reproduces the result $c^* = a$ as anticipated, and $\lambda \rightarrow 0$, which corresponds to $\pi_f(x) \propto x$, gives $c^* = 2a$. Simulation results for $\lambda = 2$ and $a = 1$ are shown in Fig. 7. The simulations confirm that the transition occurs at the predicted value $c^* = \frac{4}{3}$, and the nature of the transition is the same as in the previously considered cases (compare to Figs. 2 and 5).

IV. SUMMARY AND DISCUSSION

We have analyzed the mean adaptive walk length on random fitness landscapes with a fitness gradient c and various choices for the distribution of the random fitness component. We showed that for distributions with exponential tails, D_{RAW} exhibits a continuous phase transition between a regime with $D_{\text{RAW}} \sim \ln L$ for $c < c^*$ and $D_{\text{RAW}} \sim L$ for $c > c^*$. For distributions that decay more slowly than exponentially, $D_{\text{RAW}} \sim L$ for all $c > 0$, and for distributions decaying faster than exponentially, $D_{\text{RAW}} \sim \ln L$ for all choices of c .

Note that the distinct role of the exponential distribution in delimiting two regimes of qualitatively different behavior goes beyond the standard classification in terms of extreme value theory [30]. Intriguingly, a similar scenario appears in several other recent studies concerned with records and extremes [31–33]. In the present context the special status of the exponential distribution relies on the linear decrease of the deterministic fitness profile with the Hamming distance from the reference sequence (see Sec. III B).

The mutational pathways followed by the RAW are monotonically increasing in fitness, and a number of papers have explored the conditions for the existence of such selectively accessible paths [12, 34, 35]. In particular, in [35] it was proven that accessible paths to the reference sequence \mathcal{C}_r exist in the RMF with a probability approaching unity for $L \rightarrow \infty$ and any $c > 0$. The present work shows, however, that the dynamic significance of such pathways depends subtly on the tail properties of the fitness distribution, and for heavy-tailed distributions they are essentially irrelevant for any c . The tail also determines the behavior of the number of maxima of the RMF landscapes for large L , which converge to that of an uncorrelated random landscape for any $c > 0$ when the tail is heavier than exponential [13].

Being a parameter of the fitness landscape, the strength of the fitness gradient c governing the phase transition cannot be easily tuned in an evolution experiment. Nevertheless, the existence of two phases in which adaptive walk lengths are proportional to $\ln L$ or L , respectively, is of considerable biological importance, because for realistic genome sizes L is vastly larger than $\ln L$. A recent numerical study addressing the evolutionary benefit of recombination has found that these phases persist also for genetically diverse populations where the SSWM approximations do not apply [36]. As the advantage of recombination is determined by how far a population can adapt before being trapped at a local fitness maximum, the existence of the phase of long adaptive walks shows that a substantial advantage is possible even if the landscape is quite rugged.

Finally, we note that the RAW dynamics considered in this paper is equivalent to a zero temperature Metropolis dynamics [18], where genotypes \mathcal{C} are interpreted as configurations of L spins with energies $-W(\mathcal{C})$ assigned according to the random energy model in an external

magnetic field c [37]. In that context we predict a novel kinetic phase transition as a function of field strength from a low-field phase where the system gets stuck in a metastable state after $O(\ln L)$ spin flips to a high-field phase where a finite fraction of spins attain their ground state orientation. Our results thus apply to aging processes in spin glasses, where rigorous analysis has so far been restricted to the (less realistic) Glauber dynamics in the absence of an external field and the energy distribution is always assumed to be Gaussian [38].

ACKNOWLEDGMENTS

S.-C.P. acknowledges the support by the Basic Science Research Program through the National Research Foundation of Korea (NRF) funded by the Ministry of Education, Science and Technology (Grant No. 2011-0014680), by The Catholic university of Korea, Research Fund, 2014, and by the University of Cologne within the Center of Excellence “Quantum Matter and Materials.” J.K. acknowledges the kind hospitality of the Simons Institute for the Theory of Computing, Berkeley, during the completion of this work, and all authors acknowledge support by Deutsche Forschungsgemeinschaft within SFB 680, SFB TR12, SPP 1590, and BCGS.

Appendix A: Derivation of Eq. (8)

In this section, we show that Eq. (8) solves the recursion relation Eq. (6) for $f(y) = e^{-y}$. Since

$$\begin{aligned} \int_{-\infty}^{\infty} Q_{l+1}(y)dy &= \int_{-\infty}^{\infty} \frac{Q_l(x)}{1 - F(x - c)} dx \int_{x-c}^{\infty} f(y)dy \\ &= \int_{-\infty}^{\infty} Q_l(x)dx = \int_{-\infty}^{\infty} Q_0(x)dx = 1, \end{aligned} \quad (\text{A1})$$

for any $f(x)$, $Q_l(y)$ is normalized for any l and for any $f(x)$. Note that if L is finite,

$$\begin{aligned} H_{l+1} &= \int_{-\infty}^{\infty} Q_{l+1}(y, L)dy \\ &= \int_{-\infty}^{\infty} Q_l(x, L) \frac{1 - F(x - c)^{L-l}}{1 - F(x - c)} dx \int_{x-c}^{\infty} f(y)dy \\ &= H_l - \int_{-\infty}^{\infty} Q_l(x, L) F(x - c)^{L-l} dx, \end{aligned} \quad (\text{A2})$$

which is Eq. (4)

Since $1 - F(x - c) = e^{c-x}$ for $x > c$ and 1 for $x < c$, Eq. (6) can be rewritten as

$$Q_{l+1}(y) = e^{-y} \int_0^c Q_l(x)dx + e^{-y-c} \int_c^{y+c} e^x Q_l(x)dx, \quad (\text{A3})$$

with $Q_0(y) = e^{-y}$. One can easily find Q_1 and Q_2 such that

$$e^y Q_1(y) = 1 - e^{-c} + e^{-c} y, \quad (\text{A4})$$

$$e^y Q_2(y) = \frac{1}{2} e^{-2c} y^2 + e^{-c} (e^{-c}(c-1) + 1) y - ce^{-2c} - e^{-c} + 1, \quad (\text{A5})$$

which suggests that $Q_m(y)$ should take the form $e^{-y} j_m(y)$ with

$$j_m(y) = \sum_{k=0}^m \frac{a_{m,k}}{k!} y^k. \quad (\text{A6})$$

This is a polynomial function of order m . Since $Q_0(y) = e^{-y}$, $a_{0,0} = 1$. Due to the normalization condition Eq. (A1), the sum of $a_{m,k}$ over all k for fixed m should be 1; that is, $\sum_{k=0}^m a_{m,k} = 1$.

From Eq. (A3), we get

$$j_{m+1}(y) = e^{-c} \sum_{n=1}^{m+1} \frac{y^n}{n!} \sum_{k=n-1}^m a_{m,k} \frac{c^{k+1-n}}{(k+1-n)!} + \sum_{k=0}^m a_{m,k} \left(1 - e^{-c} \sum_{n=0}^k \frac{c^n}{n!} \right), \quad (\text{A7})$$

which yields a recursion relation for $a_{m,n}$ such that

$$a_{m+1,0} = 1 - e^{-c} \sum_{k=0}^m a_{m,k} \sum_{n=0}^k \frac{c^n}{n!}, \quad (\text{A8})$$

$$a_{m+1,n} = e^{-c} \sum_{k=n-1}^m a_{m,k} \frac{c^{k+1-n}}{(k+1-n)!}. \quad (\text{A9})$$

Note that

$$\begin{aligned} e^c \sum_{n=1}^{m+1} a_{m+1,n} &= \sum_{n=1}^{m+1} \sum_{k=n-1}^m a_{m,k} \frac{c^{k+1-n}}{(k+1-n)!} \\ &= \sum_{k=0}^m a_{m,k} \sum_{n=1}^{k+1} \frac{c^{k+1-n}}{(k+1-n)!} \\ &= \sum_{k=0}^m a_{m,k} \sum_{s=0}^k \frac{c^s}{s!} = e^c (1 - a_{m+1,0}), \end{aligned} \quad (\text{A10})$$

which again confirms the normalization condition Eq. (A1).

To obtain $a_{m,k}$ for any m, k , we first find the explicit solutions for $n = m, m-1, m-2$, and $m-3$ using Eq. (A9) and then make an ansatz for $a_{m,k}$. Setting $n = m+1$, Eq. (A9) becomes $a_{m+1,m+1} = e^{-c} a_{m,m}$, which gives $a_{m,m} = e^{-cm}$ with $a_{0,0} = 1$. Rewriting Eq. (A9) as

$$e^{c(m+1)} a_{m+1,m+1-k} = e^{cm} a_{m,m-k} + e^{cm} \sum_{p=1}^k a_{m,m-k+p} \frac{c^p}{p!}, \quad (\text{A11})$$

which gives

$$e^{cl} a_{l,l-k} = e^{ck} a_{k,0} + \sum_{m=k}^{l-1} \sum_{p=1}^k e^{cm} a_{m,m-k+p} \frac{c^p}{p!}, \quad (\text{A12})$$

one can easily find $a_{l,l-k}$ after solving $a_{l,l-m}$ for $m = 0, 1, \dots, k-1$. For example,

$$a_{m,m-1} = e^{-c(m-1)} + e^{-mc}((m-1)c-1), \quad (\text{A13})$$

$$a_{m,m-2} = e^{-cm} \left(c^2 \frac{m(m-2)}{2} - (m-1)c \right) + e^{-c(m-1)} ((m-2)c-1) + e^{-c(m-2)}, \quad (\text{A14})$$

$$a_{m,m-3} = \left(\frac{m^2(m-3)}{6} c^3 - \frac{m(m-2)}{2} c^2 \right) e^{-cm} + e^{-c(m-1)} \left(\frac{(m-1)(m-3)}{2} c^2 - c(m-2) \right) + e^{-c(m-2)} (c(m-3)-1) + e^{-c(m-3)}. \quad (\text{A15})$$

The above solutions of $a_{m,k}$ for specific k 's suggest the general form

$$a_{m,0} = 1 - \sum_{p=0}^{m-1} b_1^{m-p}, \quad (\text{A16})$$

$$a_{m,k} = \sum_{p=0}^{m-k} (b_k^{m-p} - b_{k+1}^{m-p}), \quad (\text{A17})$$

where

$$b_k^n = e^{-cn} \frac{n^{n-k-1} k}{(n-k)!} c^{n-k} \quad (\text{A18})$$

with the convention $b_k^n = 0$ for $k > n$. We first show that Eqs. (A16) and (A17) satisfy the normalization condition:

$$\sum_{k=1}^m a_{m,k} = \sum_{p=0}^{m-1} \sum_{k=1}^{m-p} (b_k^{m-p} - b_{k+1}^{m-p}) = \sum_{p=0}^{m-1} b_1^{m-p}, \quad (\text{A19})$$

which combined with Eq. (A16) meets the normalization condition. In the above calculation, we have changed the order of sum in such a way that $\sum_{k=1}^m \sum_{p=0}^{m-k} = \sum_{p=0}^{m-1} \sum_{k=1}^{m-p}$.

Now we have to verify that Eq. (A17) indeed solves Eq. (A9). To this end, it is convenient to use the identity

$$A_{k,n}^q \equiv b_k^q \frac{e^{-c} c^{k+1-n}}{(k+1-n)!} = \frac{q+1}{nq} b_n^{q+1} k B_{k+1-n}^{q+1-n} \left(\frac{1}{q+1} \right), \quad (\text{A20})$$

where

$$B_n^N(x) = \binom{N}{n} (1-x)^{N-n} x^n. \quad (\text{A21})$$

Using

$$\sum_{k=n-1}^q k B_{k+1-n}^{q+1-n} \left(\frac{1}{q+1} \right) = \frac{nq}{q+1}, \quad (\text{A22})$$

we get

$$\sum_{k=n-1}^{m-p} A_{k,n}^{m-p} = b_n^{m+1-p}. \quad (\text{A23})$$

Finally, we can prove the validity of Eq. (A9) as

$$\begin{aligned} & \sum_{k=n-1}^m \sum_{p=0}^{m-k} \left(A_{k,n}^{m-p} - A_{k+1,n+1}^{m-p} \right) \\ &= \sum_{p=0}^{m+1-n} \sum_{k=n-1}^{m-p} \left(A_{k,n}^{m-p} - A_{k+1,n+1}^{m-p} \right) \\ &= \sum_{p=0}^{m+1-n} \left(b_n^{m+1-p} - b_{n+1}^{m+1-p} \right) = a_{m+1,n}, \end{aligned}$$

which is valid for $n \geq 1$. Since the case for $n = 0$ is automatically satisfied because of Eqs. (A10) and (A19), this completes the proof.

Using Eq. (A17), we can rewrite $j_m(y)$ as

$$\begin{aligned} j_m(y) &= 1 + \sum_{k=0}^m \sum_{p=0}^{m-k} \frac{y^k}{k!} (b_k^{m-p} - b_{k+1}^{m-p}) \\ &= 1 + \sum_{n=1}^m \sum_{k=0}^n \frac{y^k}{k!} b_k^n - \sum_{n=0}^m \sum_{k=0}^n \frac{y^k}{k!} b_{k+1}^n, \quad (\text{A24}) \end{aligned}$$

where we have changed the order of sums and we have set $n = m - p$. Since

$$\begin{aligned} \sum_{k=0}^n \frac{y^k}{k!} b_k^n &= e^{-cn} \frac{y(cn)^{n-1}}{n!n} \sum_{k=0}^n k \binom{n}{k} \left(\frac{y}{cn} \right)^{k-1} \\ &= \frac{(cn+y)^{n-1}}{e^{cn} n!} y, \quad (\text{A25}) \end{aligned}$$

and

$$\begin{aligned} \sum_{k=0}^n \frac{y^k}{k!} b_{k+1}^n &= \frac{e^{-cn} c (cn)^{n-2}}{(n-1)!} \sum_{k=0}^{n-1} (k+1) \binom{n-1}{k} \left(\frac{y}{nc} \right)^k \\ &= e^{-cn} \frac{(y+cn)^{n-2}}{(n-1)!} (y+c), \quad (\text{A26}) \end{aligned}$$

we get

$$j_m(y) = \sum_{n=0}^m \frac{(y+cn)^{n-2}}{n!e^{cn}} [y^2 + (c-1)ny - nc], \quad (\text{A27})$$

which gives

$$\begin{aligned} Q_l(y) &= \sum_{n=0}^l \frac{(y+cn)^{n-2}}{n!e^{cn+y}} [y^2 + (c-1)ny - nc] \\ &= -\frac{d}{dy} \left(\sum_{n=0}^l \frac{y(y+cn)^{n-1}}{n!} e^{-y-cn} \right), \quad (\text{A28}) \end{aligned}$$

which is Eq. (8). By substitution, one can easily check that Eq. (A28) indeed solves Eq. (A3).

Appendix B: Mean and standard deviation of $Q_l(y)$

In this section, we calculate the mean z_l and the standard deviation σ_l of $Q_l(y)$. For convenience we introduce ξ_l and Ξ_l , which are defined as

$$\begin{aligned} \xi_l &= \int_0^\infty y [Q_l(y) - Q_{l-1}(y)] dy, \\ \Xi_l &= \int_0^\infty y^2 [Q_l(y) - Q_{l-1}(y)] dy. \quad (\text{B1}) \end{aligned}$$

Obviously,

$$z_l = 1 + \sum_{m=1}^l \xi_l, \quad \sigma_l = \left(2 + \sum_{m=1}^l \Xi_l - z_l^2 \right)^{1/2}. \quad (\text{B2})$$

After an integration by parts, we obtain

$$\begin{aligned} \xi_l &= \int_0^\infty y \frac{(y+cl)^{l-1}}{l!} e^{-y-cl} dy \\ &= \frac{(cl)^{l+1} e^{-cl}}{l!} \int_0^\infty t e^{-ct} e^{(l-1)(\ln(1+t)-ct)} dt \end{aligned}$$

which is Eq. (9b) and

$$\begin{aligned} \xi_l &= 1 - c - \int_{-cl}^0 y \frac{(y+cl)^{l-1}}{l!} e^{-y-cl} dy \\ &= 1 - c - \frac{(cl)^{l+1} e^{-cl}}{l!} \int_{-1}^0 t e^{-ct} e^{(l-1)(\ln(1+t)-ct)} dt, \end{aligned}$$

which is Eq. (9c). Likewise, we get

$$\begin{aligned} \Xi_l &= 2 \int_0^\infty y^2 \frac{(y+cl)^{l-1}}{l!} e^{-y-cl} dy \\ &= 2 \frac{(cl)^{l+2} e^{-cl}}{l!} \int_0^\infty t^2 e^{-ct} e^{(l-1)(\ln(1+t)-ct)} dt \quad (\text{B3}) \end{aligned}$$

which is suitable to analyze for $c > 1$. For $c < 1$, it is convenient to analyze

$$\begin{aligned} \Xi_l &= 2l(1-c)^2 + 2 - 2 \frac{(cl)^{l+2} e^{-cl}}{l!} \\ &\quad \times \int_{-1}^0 t^2 e^{-ct} e^{(l-1)(\ln(1+t)-ct)} dt. \quad (\text{B4}) \end{aligned}$$

Since

$$\begin{aligned} y \frac{(y+l)^{l-1}}{l!} e^{-y-l} &= -\frac{d}{dy} \left[\frac{(y+l)^l}{l!} e^{-y-l} \right], \\ y^2 \frac{(y+l)^{l-1}}{l!} e^{-y-l} &= -\frac{d}{dy} \left[y \frac{(y+l)^l}{l!} e^{-y-l} \right] \\ &\quad + \frac{(y+l)^l}{l!} e^{-y-l}, \quad (\text{B5}) \end{aligned}$$

ξ_l and Ξ_l , for $c = 1$, become

$$\xi_l|_{c=1} = - \int_0^\infty \frac{d}{dy} \left[\frac{(y+l)^l e^{-(y+l)}}{l!} \right] dy = \frac{l^l e^{-l}}{l!}, \quad (\text{B6})$$

$$\begin{aligned} \Xi_l|_{c=1} &= 2 \int_0^\infty \frac{(y+l)^l}{l!} e^{-y-l} dy \\ &= 2 \frac{l^{l+1} e^{-l}}{l!} \int_0^\infty e^{l(\ln(1+t)-t)} dt \\ &\sim 2 \sqrt{\frac{l}{2\pi}} \int_0^\infty e^{-lt^2/2} dt = 1, \end{aligned} \quad (\text{B7})$$

where we have used $\ln(1+t) - t \approx -t^2/2$ for small t .

Using the same method to arrive at Eq. (11) for the asymptotic behavior of ξ_l , we get for $c < 1$

$$\Xi_l \sim 2l(1-c)^2 + 2 - 2 \frac{l^l e^{-l}}{l!} e^{-l(c-1-\ln c)} \frac{c^2}{l(1-c)^3} \quad (\text{B8})$$

and for $c > 1$

$$\Xi_l \sim 2 \frac{l^l e^{-l}}{l!} e^{-l(c-1-\ln c)} \frac{c^2}{l(1-c)^3}. \quad (\text{B9})$$

To sum up, we obtain

$$z_l \sim \begin{cases} (1-c)l, & c < 1, \\ \sqrt{2l/\pi}, & c = 1, \\ \text{finite}, & c > 1. \end{cases} \quad \sigma_l \sim \begin{cases} O(\sqrt{l}), & c \leq 1, \\ \text{finite}, & c > 1. \end{cases} \quad (\text{B10})$$

Appendix C: Numerical measurement of D_{RAW}

In order to verify our analytical predictions and check whether they are still valid when we lift the restriction that RAWs should only move towards the reference sequence, we performed numerical simulations. These were carried out as follows. Before the first step, the population is positioned at “height” $h = 0$ and it is assigned a fitness value $W_0 = \eta_0$, where η_0 is drawn from the considered distribution $f(\eta)$. By height we mean the Hamming distance from the antipodal sequence. For each step, a new neighborhood consisting of L states is drawn. To each of the $L - h$ states in the forward direction (at height $h + 1$), a fitness value is assigned, which is drawn according to $W_i = (h + 1)c + \eta_i$. Correspondingly, the h backwards neighbors (at height $h - 1$) obtain fitness values according to $W_i = (h - 1)c + \eta_i$. To speed up the simulations, the fitnesses are assigned to the neighboring states in a random order until a fitness value larger than the one selected after the last step is generated. Then the population is transferred to the corresponding state and the height is updated. The walk terminates when there are no neighbors satisfying the condition on the fitness. The walk length D_{RAW} is estimated by averaging the number of steps performed up to this point, n_{steps} , over ensembles of RAW’s. For the data presented here,

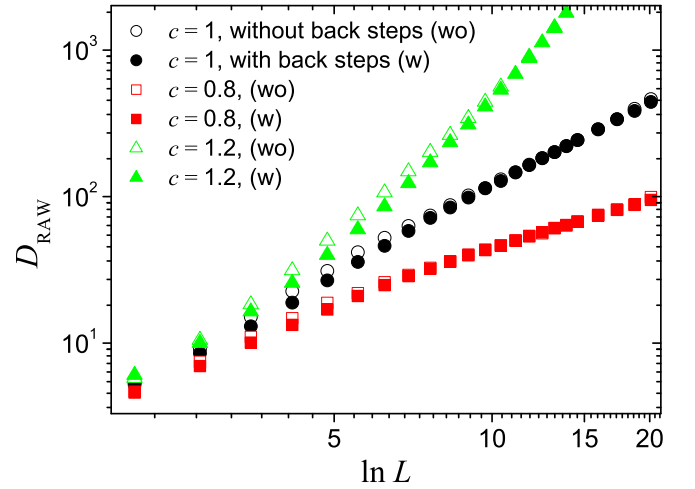


FIG. 8. (Color online) Comparison of D_{RAW} vs L for simulations with and without back steps. As can be verified, curves show excellent agreement for $\ln L > 10$ ($L > 2 \times 10^5$).

we considered ensembles of 10^3 to 10^5 walks. Note that, in order to be able to simulate large landscapes, previously encountered fitness values and the information about which states are neighbors are not stored. However, for large L this should not considerably alter the measured values of D_{RAW} .

In Fig. 8, we compared simulations with (w) and without (wo) backward steps for the case of $F(x) = 1 - e^{-x}$ for various choices of c . All curves show excellent agreement for sufficiently large $L > 10^6$, which shows that our analytical results remain valid for the original model that includes back steps.

If L is extremely large (note that the largest L in Fig. 2 is 10^{300}), even deciding a fitness of the first step by the above procedure is infeasible because we have to generate L random numbers. Therefore, direct simulation of Eq. (2) is used to simulate RAWs without back steps. The algorithm is as follows: Assume that the walker is located at “height” h . Since the walker can take a next step with probability $P_{\text{walk}} = 1 - F(x - c)^{L-h}$, a single random number generation is necessary to decide whether it stops there. When calculating $F(x - c)$ for very large x , one should be very careful if $1 - F(x - c)$ is smaller than the machine accuracy. For example, if one uses a double precision calculation, $1 - F(x - c)$ should be larger than 10^{-16} ; otherwise, $1 - [1 - F(x - c)]$ will be regarded as 1 by a computer, which gives $1 - F(x - c)^{L-h} = 0$. (Note that $(1 - 10^{-20})^{10^{200}}$ is almost zero but careless computation will give 1.) In case $1 - F(x - c)$ is very small [in our simulations, “very small” means $1 - F(x - c) < 10^{-10}$], we approximate P_{walk} as

$$\begin{aligned} P_{\text{walk}} &= 1 - e^{(L-h) \ln(1-[1-F(x-c)])} \\ &\approx 1 - e^{-(L-h)[1-F(x-c)]}. \end{aligned} \quad (\text{C1})$$

Once the next step is determined to be taken, we generate

a random number y from the distribution ($y > x - c$),

$$\frac{F(y) - F(x - c)}{1 - F(x - c)}. \quad (\text{C2})$$

In practice, we generate a uniformly distributed random number z , then we determine y by

$$1 - F(y) = (1 - z) [1 - F(x - c)]. \quad (\text{C3})$$

For $F(x) = 1 - e^{-x^\alpha}$,

$$y = \begin{cases} [(x - c)^\alpha - \ln(1 - z)]^{1/\alpha}, & x > c, \\ [-\ln(1 - z)]^{1/\alpha}, & 0 < x < c, \end{cases} \quad (\text{C4})$$

and for $F(x) = 1 - (1 + \kappa x)^{-1/\kappa}$ ($\kappa > 0$),

$$y = \begin{cases} \frac{1}{\kappa} \left(\frac{1 + \kappa(x - c)}{(1 - z)^\kappa} - 1 \right), & x > c, \\ \frac{1}{\kappa} \left(\frac{1}{(1 - z)^\kappa} - 1 \right), & x < c. \end{cases} \quad (\text{C5})$$

To obtain z_l via simulations, all we have to do is to get y from Eq. (C3) without considering P_{walk} in Eq. (C1).

-
- [1] J. A. G. M. de Visser and J. Krug, *Nat. Rev. Genet.* **15**, 480 (2014).
- [2] I. G. Szendro, M. F. Schenk, J. Franke, J. Krug, and J. A. G. M. de Visser, *J. Stat. Mech.* (2013) P01005.
- [3] M. C. Whitlock, P. C. Phillips, F. B.-G. Moore, and S. J. Tonsor, *Annu. Rev. Ecol. Syst.* **26**, 601 (1995).
- [4] J. H. Gillespie, *Theor. Popul. Biol.* **23**, 202 (1983).
- [5] J. H. Gillespie, *Evolution* **38**, 1116 (1984).
- [6] H. A. Orr, *Evolution* **56**, 1317 (2002).
- [7] H. A. Orr, *Nat. Rev. Genet.* **6**, 119 (2005).
- [8] D. R. Rokyta, P. Joyce, S. B. Caudle, and H. A. Wichman, *Nat. Genet.* **37**, 441 (2005).
- [9] S. E. Schoustra, T. Bataillon, D. R. Gifford, and R. Kassen, *PLoS Biol.* **7**, e1000250 (2009).
- [10] D. R. Rokyta, Z. Abdo, and H. A. Wichman, *J. Mol. Evol.* **69**, 229 (2009).
- [11] T. Aita, H. Uchiyama, T. Inaoka, M. Nakajima, T. Kokubo, and Y. Husimi, *Biopolymers* **54**, 64 (2000).
- [12] J. Franke, A. Klözer, J. A. G. M. de Visser, and J. Krug, *PLoS Comput. Biol.* **7**, e1002134 (2011).
- [13] J. Neidhart, I. G. Szendro, and J. Krug, *Genetics* **198**, 699 (2014).
- [14] J. Neidhart, I. G. Szendro, and J. Krug, *J. Theor. Biol.* **332**, 2018 (2013).
- [15] Note that the random fitness components remain unchanged during the adaptive walk; that is, the random variables are quenched.
- [16] S. Kauffman and S. Levin, *J. Theor. Biol.* **128**, 11 (1987).
- [17] C. A. Macken and A. S. Perelson, *Proc. Nat. Acad. Sci. USA* **86**, 6191 (1989).
- [18] H. Flyvbjerg and B. Lautrup, *Phys. Rev. A* **46**, 6714 (1992).
- [19] K. Jain, *Europhys. Lett.* **96**, 58006 (2011).
- [20] K. Jain and S. Seetharaman, *Genetics* **189**, 1029 (2011).
- [21] J. Neidhart and J. Krug, *Phys. Rev. Lett.* **107**, 178102 (2011).
- [22] S. Seetharaman and K. Jain, *Evolution* **68**, 965 (2014).
- [23] H. A. Orr, *Genetics* **163**, 1519 (2003).
- [24] H. H. Chou, H. C. Chiu, N. F. Delaney, D. Segré, and C. J. Marx, *Science* **332**, 1190 (2011).
- [25] A. I. Khan, D. M. Dinh, D. Schneider, R. E. Lenski, and T. F. Cooper, *Science* **332**, 1193 (2011).
- [26] T. Wiehe, *Genet. Res. Camb.* **69**, 127 (1997).
- [27] S. C. Park, D. Simon, and J. Krug, *J. Stat. Phys.* **138**, 381 (2010).
- [28] M. Kimura, *Genetics* **47**, 713 (1962).
- [29] J. B. S. Haldane, *Proc. Camb. Philos. Soc.* **23**, 838 (1927).
- [30] L. de Haan and A. Ferreira, *Extreme Value Theory: An Introduction* (Springer, New York, 2006).
- [31] S. Sabhapandit and S. N. Majumdar, *Phys. Rev. Lett.* **98**, 140201 (2007).
- [32] J. Franke, G. Wergen, and J. Krug, *Phys. Rev. Lett.* **108**, 064101 (2012).
- [33] G. Wergen, D. Volovik, S. Redner, and J. Krug, *Phys. Rev. Lett.* **109**, 164102 (2012).
- [34] S. Nowak and J. Krug, *Europhys. Lett.* **101**, 66004 (2013).
- [35] P. Hegarty and A. Martinsson, *Adv. Appl. Prob.* **24**, 1375 (2014).
- [36] S. Nowak, J. Neidhart, I. G. Szendro, and J. Krug, *PLOS Comp. Biol.* **10**, 1003836 (2014).
- [37] B. Derrida, *Phys. Rev. B* **24**, 2613 (1981).
- [38] G. B. Arous, A. Bovier, and V. Gaynard, *Phys. Rev. Lett.* **88**, 087201 (2002).